Research on Geometrical Modeling and Physical Properties of Porous Structure of Human Bone

Wang Tiansu[1]

[1]High School Affiliate to Shanghai Jiao Tong University, Shanghai, China.

Keywords:

Bionic structure
Bone pore
bionic modeling
fractal geometry
Three-dimensional printing

ABSTRACT

Bionic structures have been proved useful for its high strength-mass ratio in the field of medicine and aerospace. However, in standard engineering structures, bionic counterparts have not been prevailed. This paper provided a simple method of bone micro-structure modeling and computer production, which solved the problem that commercial CAD software could not support graphic modeling of analytical characteristics. The boundary of pore structure in bone tissue was obtained by CT images of human bones. The fractal dimension of the pore structure was calculated, the skeleton pore contour graph group with self-similar fractal characteristics was obtained, and the mmodel of bionic characteristics of internal pore structure was established. The fitted pore structure contours with different shapes were randomly arranged in the selected area to obtain the required void ratio of the area. Two constraints, pore capillary characteristic model with self-lubricating effect and 3D printing resolution, were introduced to generate the two-dimensional structure of bone bionic features, and then the three-dimensional structure was generated by stretching, thus completing the three-dimensional design of bone tissue pore bionic structure. The three-dimensional bionic structure was applied to the universal joint design of a snake-like robot, and the corresponding parameters such as the porosity of bone pore structure were modified according to its mechanical performance requirements, to obtain a bionic mechanical structure with excellent strength/weight ratio and self-lubricating characteristics. The ultimate rotation angle of the universal joint with bionic structure is five degrees larger than that of the Hooke hinge. . The volume of the universal joint with bionic structure is $11.79 \pm 4.3\text{e-}06$ cubic centimeters, which is lower than that of the original Hooke hinge($20.43 \pm 1.1\text{e-}05$ cubic centimeters). Thus, the universal joint with bionic structure reduces the weight as well as advances the freedom of snake-like robot.

Corresponding Author:

Wang Tiansu,
High School Affiliate to Shanghai Jiao Tong University,
Shanghai, China.
Email: tswang0410@163.com

1. INTRODUCTION

The prevailed problems of standard engineering structures include lack in durability and qualified strength-mass ratio. In contrast, biological structures consist of self-lubricating structures advancing wearing resistance and flexibility of biological structures. Biological structures also contain porous structure reducing mass while remaining strength. The research goal of this paper is to build a bionic model for the pore structure of human bones and apply the bionic structure to flexible engineering structures that require strength-to-mass ratio and self-lubrication, such as spherical hinge joints of snake-like robots.

1.1 Related research and theory

At present, in-depth research has been carried out in bone bionic modeling in the research community to obtain higher-performance material structures. Most of these studies focus on the bionic design of implant tissues and the synthesis of bionic materials. In Ref[1], Qu et al. proposed a bionic modeling method for the fractal structure of bones. The authors used Grasshopper and other plug-ins to construct a fractal porous scaffold similar to the fractal dimension of the Koch curve and simulated the decreasing bone porosity from cancelous bone to cortical bone by controlling the iterative series of a porous scaffold. In this paper, the author mentioned that this bionic structure can show its advantages in radial porosity, mechanical properties, and permeability. In Ref[2], Chen et al.. mentioned the modeling method of microscopic porous structure mimicking the cross-section of the bone. In this paper, the edges of pores are extracted from the CT image of a human skeleton cross-section, the pore structure is fitted by the spline function, and the fitted spline curve is generated randomly. It is proved that the porous structure of human bone has a fractal self-similar structure. Through self-similarity, the pore generation model of bionic bone is obtained, and the bionic structure is used in the design of human prosthesis bone so that prosthesis can better promote the growth and recovery of human bone tissue. In Ref[3], Gu et al. proposed a new bionic soft landing mechanism model by imitating the leg muscle structure of cats. The author uses pneumatic muscle as the main energy-absorbing material and aluminum alloy mechanism to establish a cat-like soft landing buffer mechanism model.

It can be seen from the CT image of the cross-section of the bone that the interior of the bone is composed of many micropores. The key technology for the microscopic bionic design of the human skeleton is to establish a model that can effectively describe the pore structure and connector and describe the pore structure and its distribution.

The research on the microstructure and mechanical properties of bionic bones has also become an academic hotspot. Shao and Xu mentioned in Ref[4] that according to the existing bone quality research, the factors affecting the mechanical properties of bone include its macro and microstructure. The combination of macro and microstructure is a necessary condition for bone biomechanics. In Ref[5], Zheng and Mao mentioned that diamond-shaped textures were designed on the surface of titanium alloy artificial joints to enhance the wear resistance of titanium alloy artificial hip joints and a mathematical model of hydrodynamic lubrication of textured joint surfaces was established through Reynolds equations, thus the friction performance of bionic bones was calculated. It was concluded that bionic textures could effectively enhance the wear resistance of titanium alloy artificial hip joints. In Ref[6,7], the possibility of manufacturing bionic texture by additive manufacturing is convicted, which reflected the feasibility of manufacturing bionic structure with bone pores.

Thus, the bionic modeling of biological tissue has great application prospects in medicine and engineering and has high scientific research value.

1.2 Research motivation and purpose

From the above research results in the research community, it can be seen that bionic structures have advanced mechanical properties and can be used in aerospace, bionic robots, and other places that require high strength/weight ratio. It is also proved that the bionic structure of the human skeleton can be used in special application scenes such as self-lubrication of mechanical moving parts because of its fine characteristics such as self-lubrication and capillary effect, which are not available in conventional structures, and has high application value.

However, most research focuses on the imitation and manufacture of human skeleton microstructure. The lack of a simple and practical modeling method for human skeleton microstructure has affected the

popularization and application of this bionic structure. In application research, it is mainly aimed at the bionic research on human implants, or the usage of the bionic structure in the structural parts of aircraft with high strength/weight ratio, and it is rare to see the publication of research on applying the bionic structure to standard mechanical structures.

The goal of this paper is to study the mathematical modeling method and computer generation method of micro-pore structure in the human skeleton and find a simple and practical modeling method and three-dimensional generation method. The bionic structure of the human body is applied to the standard mechanical structure so that the research results can be widely applied. The research content also includes researching and inventing a mechanical structure with high mechanical properties, self-lubricating capillary structure characteristics, and dynamic pressure lubrication surface characteristics, and applying this structure to the spherical joint of a snake-like robot to improve the performance of the joint.
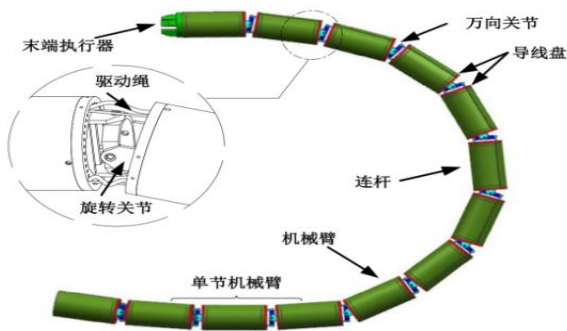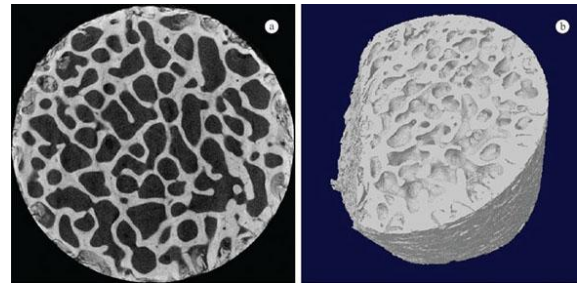

Figure 1. Snake-shaped robot

Figure 2. Cross-sectional pore structure of bone

2. RESEARCH METHOD

2.1 binarization of bone image and edge detection

Image J is used to detect the edge of the binarized CT image of the bone pore structure (Figure 2) and enhance the contour map generated by the edge. The contour map of the bone cross-section obtained is shown in Figure 3, which prepares for the fractal dimension calculation and bionic design of bone pore structure in the future.
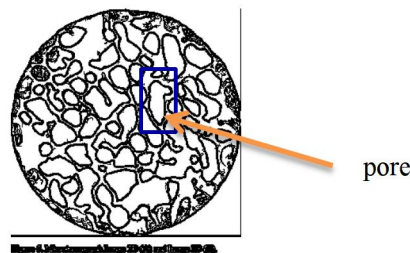

Figure 3. outline of bone cross section after image processing

2.2 Calculation of fractal dimension of bone pore structure

To effectively describe the irregularity of bone pore structure, traditional design methods are powerless, and the characteristic of fractal theory is that it can effectively find out the regularity contained in these irregular structures, thus effectively solving this problem[8]. Because the outline of the bone pore structure is an irregular closed curve, its fractal dimension can be calculated by the Slit island method. The Slit island method can calculate the fractal dimension of a closed curve by calculating the relationship between perimeter and area. For irregular graphs, the relationship between perimeter and area is as follows:

$$\alpha(\varepsilon) = \frac{P^{1/D}(\varepsilon)}{A^{1/2}(\varepsilon)}$$

where $P(\varepsilon)$ and $A(\varepsilon)$ represent the perimeter and area measured with constant length (ε), $\alpha(\varepsilon)$ represents a constant, D represents the fractal dimension of the graph.

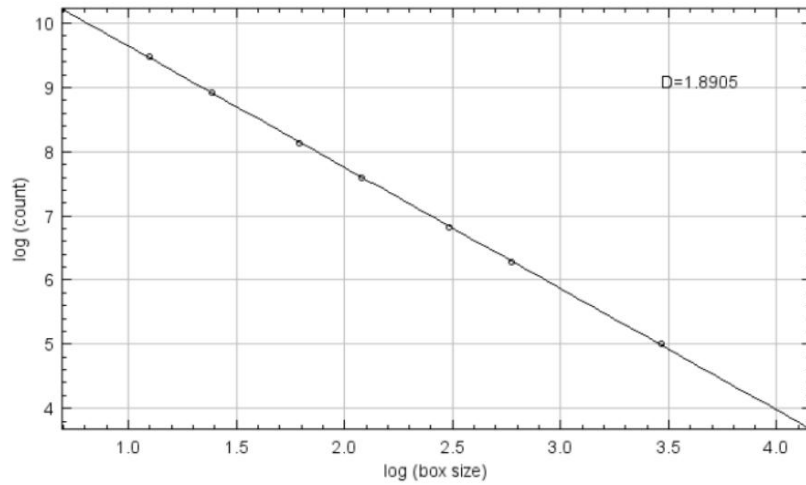If both sides take logarithms, then $\lg P(\varepsilon) = D\lg\alpha(\varepsilon) + \frac{D}{2}\lg A(\varepsilon)$

Figure 4. Log (box size) represents logarithm of total area of pores, log (count) represents logarithm of total circumference of pores, D represents the score dimension value from formula

In the calculation process, the bone pore structure graph (Figure 3) is enlarged by multiple, and the upper limit is one order of magnitude (64 times). The total perimeter of the pore structure is measured by unit length, and the total area of the pore on the image is measured by the square of unit length. Calculate the ratio of the total perimeter of pores with different magnifications to the logarithm of the total area, and make linear fitting to get the fractal dimension value of the graph. Figure 4 is the calculation result after the linear fitting of one of the pores. The irregularity of the boundary is directly related to the size of its fractal dimension D, and the larger the value of D, the more irregular the boundary is. When D is close to 1, the boundary is quite regular and orderly, and consists of many straight line segments; But with the increase of D value, the graph will become more and more irregular.
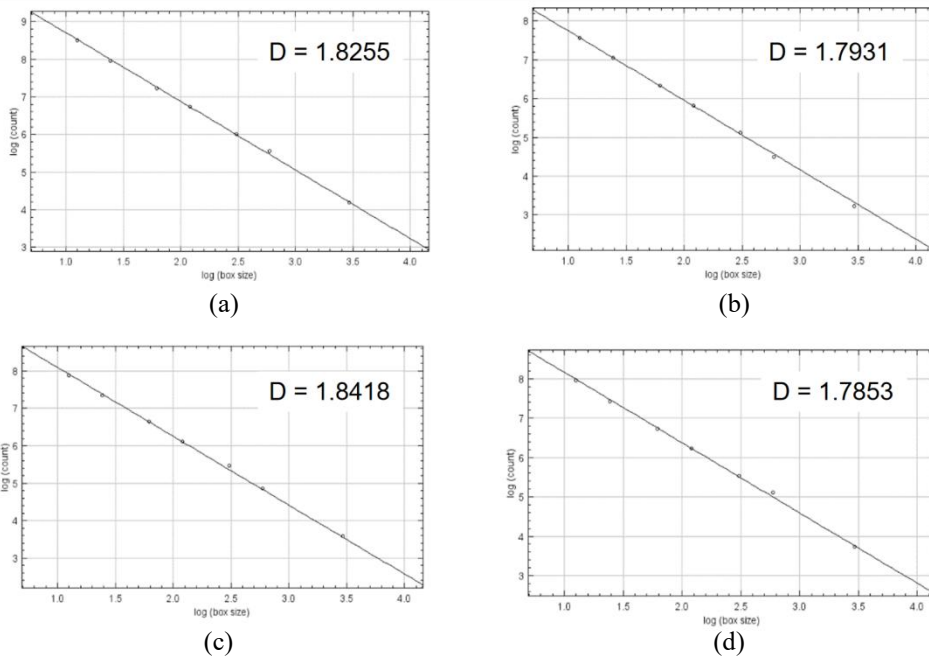

Figure 5. Calculation results of fractal dimensions of different bone pore structures.

By calculating the fractal dimensions of different pores many times, as shown in Figure 5, the fractal dimension of the pore structure of bone is about 1.8, and the difference in fractal dimensions of different

pores is about 0.05. From the above data, it can be concluded that although the fractal dimensions between bone pore structures vary, the bone pore structures have high similarity. Therefore, in the bionic design of bone pore structure, the randomness and similarity of the bionic structure should be the main focus.

2.2.1 Constraints of fractal dimension of bone pore structure on bionic design of bones
In order to simulate the pore structure inside the bone to the greatest extent, so that the generated three-dimensional structure has the best mechanical properties, the generated three-dimensional bionic structure must meet the following conditions:

1. The shape of the cross-sectional pore of the three-dimensional structure must be as close to the shape of the bone pore as possible so that the bionic structure has high similarity to the bone pore.

2. The cross-sectional pore distribution of a three-dimensional structure must be similar to that of bone, and its porosity can be adjusted according to the mechanical properties of a three-dimensional structure.

3. The cross-sectional pores of three-dimensional structures must be random in shape and size, and the randomness must be controllable, and at the same time approximate to the fractal dimension of bone pore structure.

According to the capillary phenomenon formula

$$h = \frac{2\sigma\cos\theta}{\rho g r}$$

where h represents the height of liquid elevated, r is the radius of the tubule, ρ is the density of liquid, θ is the intersection angle between the liquid surface and the pipe wall, which depends on the types of liquid and gas, the pipe wall material, and other factors. The controllable variable is the tubule radius. Therefore, to improve absorbance to lubricating oil of the bionic structure of bone pores, reduction in the pore radius should be as much as possible until reaching the minimum resolution of 3D printing.

2.2.2 Generation method of bone pore bionic structure
In order to meet the requirements of the above three-point three-dimensional bionic structure, the contours of different bone pore structures are obtained from the edge enhancement map of bone pore structure, and the B-spline closed curve is generated by Matlab to fit the contours of the selected bone pores. After importing the generated B-spline curves to Acis library which is used to geometric imitation, the plane areas are calculated respectively, the direction and size of the generated B-spline curves are randomly changed within a specific range, the generated B-spline curves are randomly filled within a specific range (as shown in Figure 6 and Figure 7, with a box as the boundary) with a certain porosity (the area ratio of the pore structure within the range), and the figures are guaranteed to be non-overlapping and evenly distributed, so as to obtain the bionic cross-section of the bone pore structure.
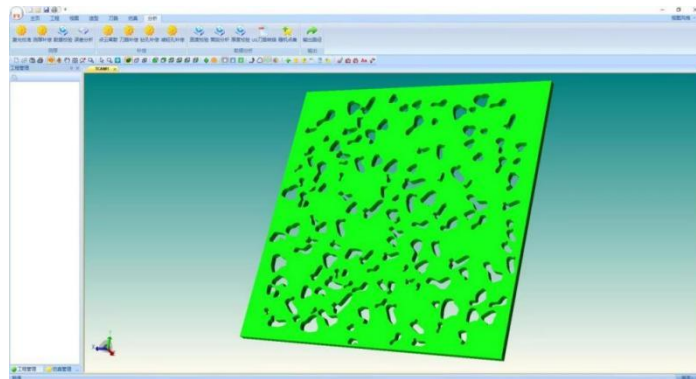

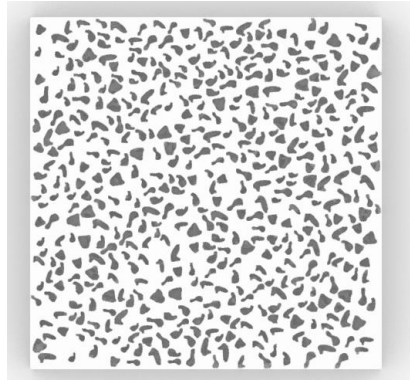Figure 6. Image generated when porosity is 30%

Figure 7. Image generated when porosity is 70%

2.3 Formation of Bone Pore Shape

The formation of B-spline control points is based on the value points of bone pore structure, which is realized by Matlab program to create B-spline. From the pores of the pore pattern, the fractal structure with similar and irregular edges is extracted, which makes the structure have an advanced strength-to-weight ratio, and has advanced adsorption and capillary effect of lubricating fluid. Figure 8 shows four representative graphic mathematical models generated by B-spline fitting.
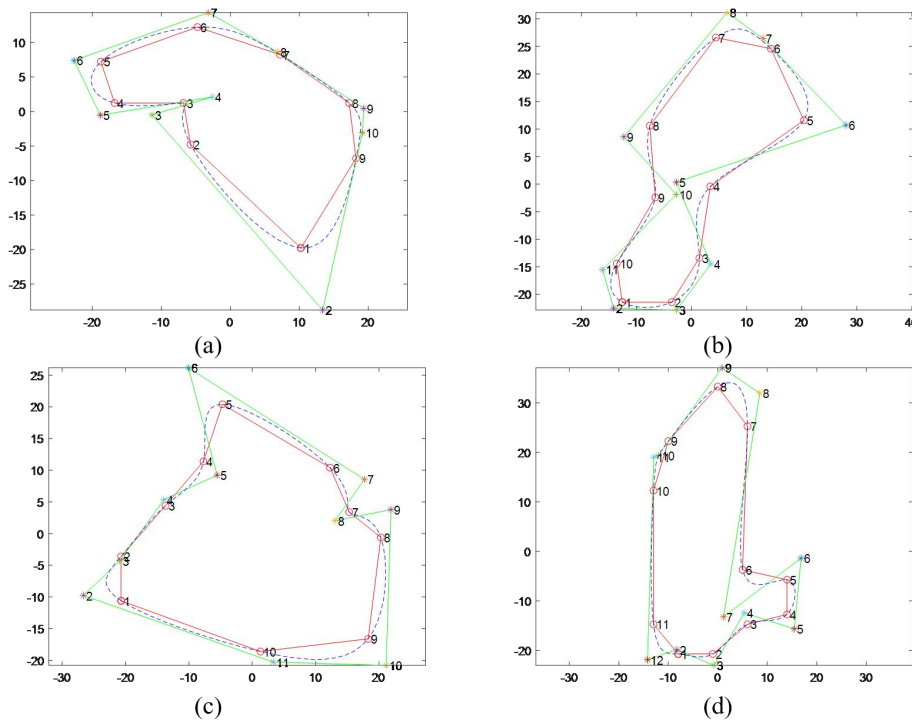

Figure 8. diagrams of typical pores generated by B-spline coded with Matlab

2.4 Random arrangement and generation of Bone Pore Structure

The generated B-spline control points are input into the software developed based on ACIS, and a closed B-spline function curve is generated in the software according to the coordinates of the control points, and the coordinates of the center point of the closed curve are generated by the four vertices with the largest and smallest X and Y coordinates. Move the center point of the curve to the origin. The distance between the control point and the origin of the B-spline function is randomly scaled to make the generated function curve random. After the B-spline curve is generated, the generated function curve is randomly moved, and the B-spline curve is surrounded by four vertices with the largest and smallest X and Y coordinates on the curve, so that U and V curves are generated in the X and Y axes respectively,

and patches with the B-spline curve as the boundary are generated by fitting. Randomly rotate the patches generated after fitting within a limited range, and make the distance between the generated new patches not less than 5 units. For each patch generated, calculate its area and accumulate it, and so on, and stop generating new patches when the total generated area reaches a specific proportion of the generation range.

The code implementation is as follows:

1. **Create a boundary:** the above code sets the vertex of the generation range of the irregular surface set by the above code, thus setting the boundary of the generation range. And generate a specific range outside the boundary. The surface data of these ranges are recorded in an array, so that the generated patch will not interfere with it, so that the generated patch will not exceed the boundary.

2. **Create a basic control point unit:** the control points of four B-spline curves fitting bone pore structure in text files which are read and introduced to prepare for generating corresponding closed curves.

3. **Scaling the basic control point unit:** the above functions are used to generate random scaling of closed curves. The principle is to connect the center point of the generated closed curve with the recorded vertex on the curve, and set the scaling multiple of the connecting line to generate a scaled new vertex and a new control point of the closed curve.

4. **The mobile control point unit:** the above code is used to move the scaled closed curve randomly with rand () function. The role of nran is to set random values. According to a specific random value, the center point of the closed curve will be randomly moved from the origin to the four quadrants. Since the set generating ranges in the X and Y axis directions are 200 respectively, the upper limit of the X and Y axis distance of random movement is 200. RanLst records the coordinates of all qualified center points, and distance is used to control the distance between any two center points to ensure that patches fitted by randomly generated center points will not interfere with each other with high probability.

5. **Find the center of the zoom translation unit:** the above code is used to find the maximum and minimum values of x and y of the curve, and then to determine the graphic boundary and calculate the center point of the curve. Its principle is to set specific parameters as a reference, and then compare the recorded curve vertices with the corresponding parameters, so as to continuously update minX, maxX, minY and maxY until a qualified point is found.

6. **Determine whether the center is out of scope:** when the x coordinate of the center point of the generated curve is greater than 200 or the y coordinate is less than -200 or greater than 200, the center point is judged by the program to be beyond the boundary range, and the loop is jumped out to regenerate the center point of the curve.

7. **Generating the outline of the patch:** the above code fits the contour line of the patch by introducing the moved B-spline closed curve control points, so as to prepare for generating the point cloud of UV curve.

8. **Generating two-dimensional point clouds of UV patches:** with the minimum value of X coordinate -2 and the maximum value of X coordinate +2 on the fitted contour as the length, the line segments are generated at the interval of 1 unit from the minimum value of Y coordinate to the maximum value of Y coordinate on the fitted contour. Divide each line segment into 500 equal parts, and record the points within 0.1 unit from the intersection of the contour and the line segment into a closest. Find the two points closest to the intersection of the contour and the line segment from the closest as the vertices of the new line segment. The new line segment is equally divided by the difference between the maximum value of the Y coordinate and the minimum value of the Y coordinate, and the equally divided points of the line segment are recorded in the PointCloud, thus obtaining the two-dimensional point cloud of UV patches.

9. **Fitting the patch according to the two-dimensional point cloud, and performing random rotation:** the above code is for UV fitting of the surface surrounded by a closed B-spline curve and rotation with dRotate as a random value.

10. **Check interference:** the above code is used to generate the interference judgment of the surface, and the inspection interference function of ACIS is cited to make the judgment. If the graph does not interfere with any surface recorded in faceLst, the graph data will be stored in faceLst for subsequent calculation of the area ratio of the graph in the generation range. If the graphics overlap, return and regenerate the graphics.

11. **Calculating Area and Ending Procedure:** accumulate the areas of qualified surfaces after interference inspection. When the total area reaches the proportion of the set area, jump out of the cycle. The program is over. The generated pores are imported into rhino7 and stretched into solids to prepare for the subsequent Boolean operation with a spherical hinge. In the subsequent experiments, the interference

judgment between pores will be changed according to the mechanical requirements (the judgment range will be narrowed or expanded, so that the pores can be more effective under the condition of ensuring the resolution), and the number of random generation will be modified (the pore density will increase with the increase of random generation times).

2.5 Utility of bionic human bones in joints of snake-like robot
2.5.1 Design of Self-lubricating Joint of Snake-like Robot
2.5.1.1 Improvement Scheme of Hooke Hinge Joint of Snake-like Robot

The original snake-like robot adopts Hooke joint, which has the disadvantages of small rotation angle (36 degrees) and low strength/weight ratio, as shown in Figure 9. In this paper, the spherical joint with self-lubricating characteristics replaces the original Hooke hinge joint to achieve a larger rotation angle and strength/weight ratio. As shown in Figure 10.
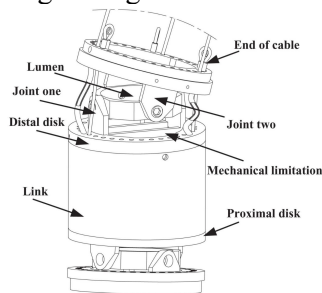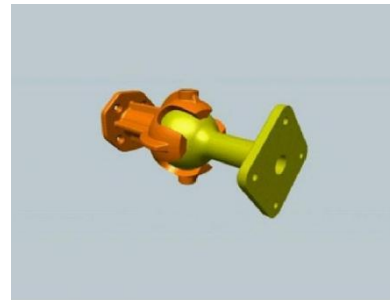

Figure 9. Hooke Hinge

Figure 10. Spherical Hinge

2.5.1.2 Design of Spherical Hinge Joint of Snake-like Robot

The assembly drawing and parts drawing of the ball joint are designed, as shown in Figure 10 and Figure 11. From the effect of the overall structural design, the rotation angle of the ball-dumpling joint can reach 42 degrees, which ensures that the snake-like robot has better flexibility. The final design of spherical hinge is shown by Figure 12 and Figure 13.
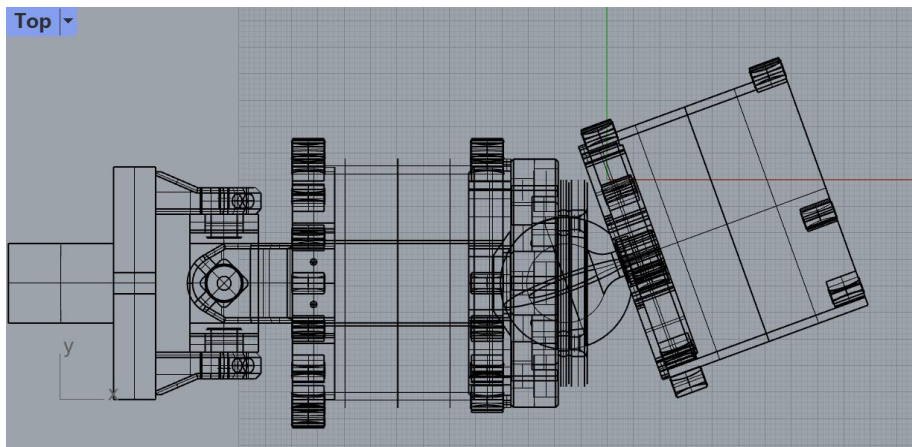

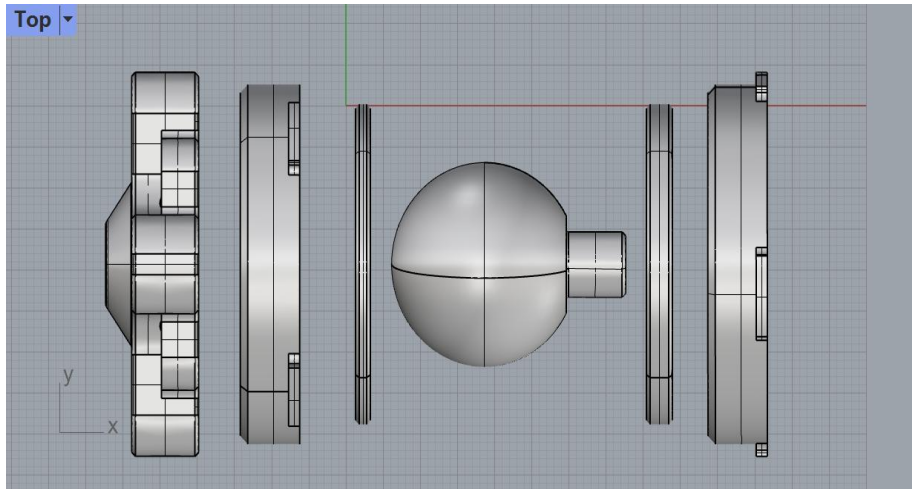Figure 11. Assembly drawing of spherical joint of snake-like robot.

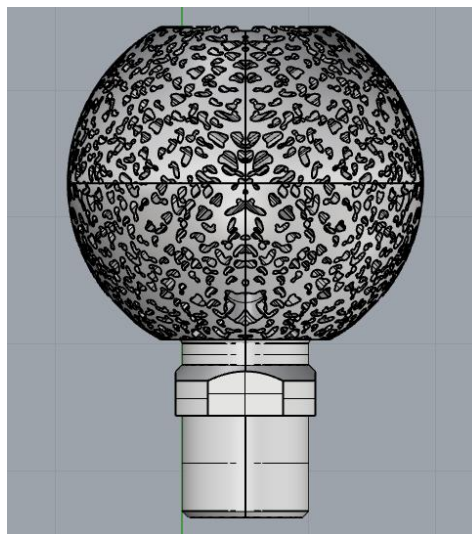Figure 12. Part drawing of spherical joint of snake-like robot.

Figure. 13. Final product of Boolean operation of spherical hinge joint and pore structure.

2.6 Manufacture of Substitute Joints

Figure 14. 3D printed product

To manufacture the pore structure on the surface of the spherical hinge, additive manufacturing is adopted as the manufacturing scheme. To ensure the printing accuracy to the greatest extent, the titanium product was printed by selective laser sintering (SLS). The minimum pore diameter of the finished product is 0.4mm, which is the limited resolution of the 3D printer.

3. RESULTS AND DISCUSSIONS
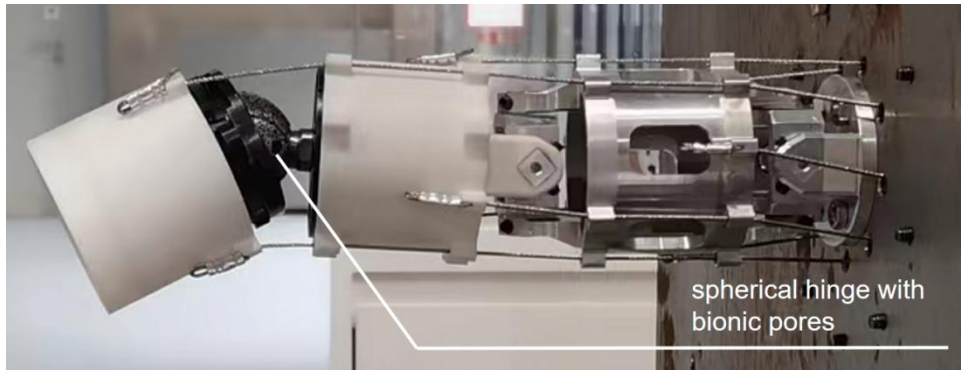### 3.1 Application of Substitute Joints

Figure 14. The bionic spherical hinge joint is applied on the snake-like robot and successfully reach a rotational angle of 42 degree

The printed titanium spherical hinge with bionic pores is applied on the snake-like robot. In the rotational experiment. The spherical joint reach a ultimate rotational angle of 42 degrees, surpassing the ultimate rotational angle of original Hooke joints on the snake-like robot (37 degrees) by 5 degrees[8]. Therefore, the flexibility of the snake-like robot is advanced. According to the volume estimation from Rhino 7, the volume of spherical hinge with bionic pores is $11.79 \pm 4.3\text{e-}06$ cubic centimeters. Comparing to the volume of the original Hooke joint ($20.43 \pm 1.1\text{e-}05$ cubic centimeters), a single joint substitution can reach a rate of lighting to 73.28 percent.
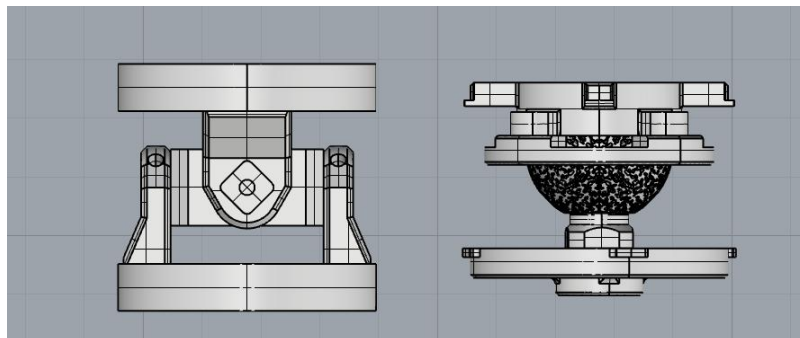

Figure 15. The original Hooke joint (left) and the spherical hinge with bionic pores (right)

3.2 Practicability of bionic porous structure

From the stage results of this research, a fast and simple modeling method is applicable to the bionic structure of the human skeleton with its self-similarity and can solve the problem of analyzing characteristic graphics that can not be solved by CAD design software. Bionic structures have advanced mechanical properties, such as self-lubrication and capillary effect, which are not available in conventional structures. They can be used in places that require high strength/weight ratio, such as aerospace and bionic robots, and can also be used in special scenes such as self-lubrication of mechanical moving parts, which has high application value. It is of great academic research value for geometric modeling of bone microstructure, especially for integrating physical effects such as self-lubrication and capillary effect into material micro-modeling and simulation modeling with process constraints of 3D printing.

4. CONCLUSION

At present, the geometric modeling of human skeleton microstructure has been completed, and the physical effects such as self-lubrication and capillary effect have been initially considered in the micro-modeling of materials. The design of the spherical joint of the snake-like robot has been completed, and

the expected results have been achieved in increasing the rotation angle. In the future, we will focus on the micro-modeling and optimization design of physical effects such as self-lubrication and capillary effect of ball dumplings, complete the 3D printing manufacturing of titanium alloy with high strength/weight ratio and self-lubrication effect, and install it in snake-like robots for application. In the later period, the new bionic structural materials developed by the project would be extended and applied to the self-lubricating devices of aviation aircraft and machinery and applied for invention patents.

REFERENCES

[1] L. Tang et al., "Design of a cable-driven hyper-redundant robot with experimental validation," *International Journal of Advanced Robotic Systems*, Vol.14, No.5, p. 172988141773445, 2017.

[2] Z. Chen et al., "Bionic design of human bone microstructure based on fractal theory," *Journal of Wuhan University of Technology*, Vol.26, No.4, April 2004.

[3] H. Gu, "Design and performance study of the soft landing mechanism of the lunar module imitating cats," *MA thesis of Harbin Institute of Technology*, Dec 2018.

[4] J. Shao et al., "Clinical research progress of biomechanical properties of bone," *Journal of logistics university of capf (Medical Edition)*, Vol.30, No.4, pp. 29-134, April 2021.

[5] Q. Zheng et al., "Analysis of hydrodynamic lubrication performance and friction reduction of bionic textured surface on artificial hip joint pair," *Journal of Mechanical Engineering*, Vol.57, No.11, pp.102-111, 2021.

[6] Y. Lv Yanjun et al., "Research progress in design, processing and application of bionic weaving pattern," *Surface Technology*, Vol.50, No.2, pp.112-122,159, 2021

[7] L. Dong et al., "Laser sintering of self-lubricating bionic micro-texture and its tribological properties," *Hot working technology*, Vol.2023, No.10, pp. 29-34, Nov 2022.

[8] L. Tang, "Study on the operational performance analysis and motion planning of snake-like robot driven by super redundant rope", *Ph.D. thesis of Shanghai Jiaotong University*, September 2019.

BIOGRAPHIES OF AUTHORS

	Educational background: High school student of High School Affiliated to Shanghai Jiaotong University Research interest: 1. Engineering Award and honor: 1. Learner of YINGCAIJIHUA